High-efficiency native-oxide-passivated high-index-contrast ridge waveguide lasers

D. Liang, J. Wang and D.C. Hall

A GaAs-based high-index-contrast ridge waveguide laser is fabricated using a self-aligned process of deep dry etching plus oxygen-enhanced wet thermal oxidation of low Al-content AlGaAs. Lasers operating at $\lambda = 813$ nm (CW, 300 K) with external differential quantum efficiencies as high as 78% are demonstrated, indicating effective passivation of the directly-oxidised etched active region sidewall surface.

Introduction: High-index-contrast (HIC) photonic devices have been of great interest recently owing to the desirable capability for increased integration and functionality [1]. Both thermally grown and deposited SiO_2 have been successfully utilised to confine light within a small-volume silicon-on-insulator (SOI) waveguide, enabling sharply bent passive devices such as ring resonators [2]. Since the discovery of wet thermal oxidation of AlGaAs in the early 1990s [3], much effort has been devoted to the development of III-V-based HIC optoelectronic active devices [4]. We have recently demonstrated a 'non-selective' technique for preferentially enhancing oxidation rates of low Al-composition $Al_xGa_{1-x}As$ ($0 < x^\circ < 0.6$) through the controlled addition of trace amounts of O_2 to the usual $N_2 + H_2O$ vapour process gases [5]. This non-selective process allows direct oxidation of a conventional AlGaAs-GaAs quantum well heterostructure active region, including the low Al-composition waveguide core layer, resulting in a HIC interface. The higher refractive indices ($n \sim 1.65$) of wet thermal native oxides of low Al-content AlGaAs grown with the participation of O_2 relative to that of conventional wet thermal oxides ($n \sim 1.55$) indicates the formation of a denser, higher quality oxide [5, 6]. In this Letter, we report a simple, self-aligned process for fabrication of HIC ridge waveguide (RWG) lasers in which the non-selective oxidation of the etched sidewall simultaneously provides effective electrical isolation, interface passivation and strong optical confinement, resulting in excellent high-efficiency diode injection laser performance.

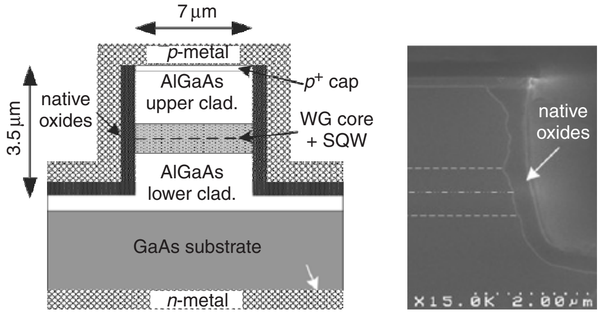

a *b*

Fig. 1 *Schematic of finished laser structure and SEM cross-section of GRINSCH laser structure after etching (with 200 nm-thick PECVD SiN_x mask layer on ridge top) and 30 min, 450°C non-selective oxidation*

a Schematic
b SEM cross-section

Device fabrication: Laser devices are fabricated in a $\lambda = 808$ nm high-power, large optical cavity, single quantum well (SQW) graded-index separate confinement heterostructure (GRINSCH) wafer structure with $Al_{0.6}Ga_{0.4}As$ waveguide cladding layers, grown via metal organic chemical vapour deposition by Epiworks, Inc. to closely match the design in [7]. After deposition and photolithographic patterning of a 200 nm-thick plasma-enhanced chemical vapour deposition SiN_x mask layer, the epilayer is dry-etched via reactive ion etching (RIE) into the lower cladding layer, forming a 3.5 µm-tall, 7.5 µm-wide ridge, and subsequently nonselectively wet oxidised at 450°C with the addition of 4000 ppm O_2 (relative to N_2 carrier gas) for 30 min. Approximately 340 nm of oxide is grown on the RWG sidewalls (and base) as shown in the scanning electron microscope image of Fig. 1*b*, where dashed lines indicate the position of the GRINSCH core and SQW. Following oxidation, the SiN_x mask is selectively removed via RIE. After standard lapping, polishing, metalisation and cleaving, unbonded devices are probe tested, junction side up, under both pulsed (0.5–1 µS pulse, 1% duty cycle) and continuous wave (CW) conditions at 300 K using a Keithley Model 2520 laser test system. The total p-side metallisation (Ti/Au) thickness is ~320 nm, and the device facets are uncoated. A schematic cross-section of the final device is shown in Fig. 1*a*. The leakage through the oxide layer is negligible (e.g. $J < 5$ nA/cm^2 at 2.5 V was measured for a 184 nm oxide).

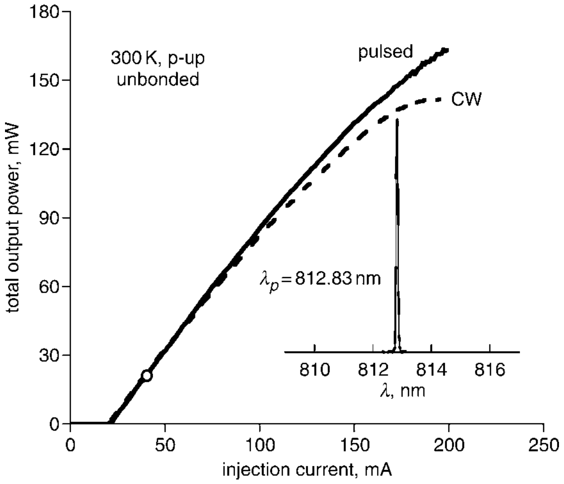

Fig. 2 *Pulsed and CW 300 K output power against current characteristics of GRINSCH high-index-contrast ridge waveguide straight stripe geometry laser with uncoated facets*

$I_{th} = 21.5$ mA; active width $w = 7$ µm; laser cavity length $L = 452$ µm; threshold current density $J_{th} = 679.5$ A/cm^2. Differential slope and external quantum efficiencies at $I = 40$ mA are $R_d = 1.19$ W/A and $\eta_d = 78\%$, respectively
Inset: Spectrum of laser operating at continuous injection current of 40 mA (marked by dot on P–I curve, $\lambda_{peak} = 812.8$ nm)

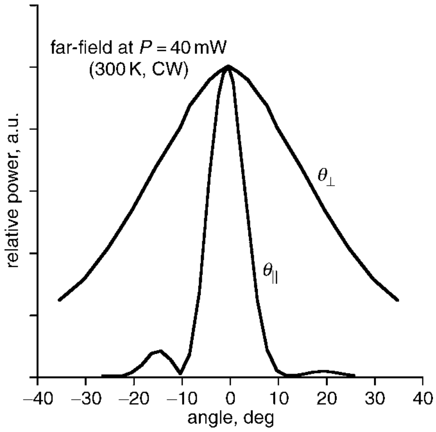

Fig. 3 *Far-field patterns in planes ($\theta_\parallel$) and normal ($\theta_\perp$) to junction plane with full-width at half-angle values of 8.8° and 43.1°, respectively*

Device performance: Fig. 2 shows the total (two facet) output power against current characteristic for a straight HIC RWG stripe geometry laser, showing a low 21.5 mA threshold current (threshold current density $J_{th} = 679.5$ A/cm^2) and a high differential responsivity of 1.19 W/A (differential quantum efficiency of $\eta_d = 78.0\%$) in both pulsed and CW mode (DC sweep time ~0.34 s) up to an injection current of 90 mA. Total wallplug power conversion efficiency at 90 mA (and 2.05 V) is 40.3% Thereafter, the unbonded, junction-up laser emission efficiency decreases owing to heating effects, decreasing to 0.58 W/A ($\eta_d = 38\%$) in pulsed mode, rolling over in CW mode at $I = 200$ mA. The spectra shown in the inset, measured at 40 mA CW (steady on), shows a single longitudinal mode of width ≤0.08 nm (limited by the optical spectrum analyser resolution). A sidemode suppression ratio of >20 dB is obtained from log data at the same injection current level (not shown). Fig. 3 shows far-field radiation patterns both parallel ($\theta_\parallel$) and normal ($\theta_\perp$) to the junction plane acquired at a total two-facet output power of 40 mW in CW mode (steady on). The measured full width at half angle of the divergence are 8.8° and 43.1° parallel and normal to the junction plane, respectively. The predominantly singlelobe pattern for $\theta_\parallel$ indicates the fundamental (lowest order) mode dominates during the lasing operation although the actual active stripe width (ridge width less total oxide thickness) of $w = 7$ µm exceeds the singlemode cutoff condition ($w \sim 1$ µm) obtained from a beam propagation method simulation on a passive waveguide with the same structure. Lasing of the higher-order modes is believed to be suppressed by their higher loss. Further studies of the power and dimension limits for singlemode operation are in progress.

Conclusions: We have fabricated high-efficiency ridge waveguide lasers with an 808 nm GaAs-based GRINSCH structure using a self-aligned process where the waveguide core and SQW active region exposed through deep dry etching is directly oxidised via a non-selective wet thermal oxidation to form a high-quality insulating and passivating native oxide yielding a high lateral refractive index step of $\Delta n = 1.7$. Using this HIC RWG structure, lasing of half-ring resonator lasers with a ring radius of curvature as small as $r = 10$ µm has been observed [8]. External differential quantum-efficiency up to 78% is achieved on the straight waveguide lasers presented here, indicating that the non-radiative recombination normally expected to occur at the semiconductor/native oxide interface is not strongly deleterious to laser performance. Elimination of lateral current spreading and the strong optical confinement provided by the deeply-etched design contribute to enhanced laser efficiency. To our knowledge, this work represents the first diode laser successfully employing an oxide (either native or deposited) to directly passivate the bipolar QW active region without significantly degraded device performance.

Acknowledgments: This research was funded by the National Science Foundation (NSF) grant ECS-0123501. D. Liang acknowledges valuable discussions with G. L. Snider at the University of Notre Dame.

6 December 2005
Electronics Letters online no: 20064090
doi: 10.1049/el:20064090

D. Liang, J. Wang and D.C. Hall (*Department of Electrical Engineering, University of Notre Dame, Notre Dame, IN 46556-5637, USA*)

E-mail: dhall@nd.edu

References

1 Chin, M.-K., Lee, C.-W., Lee, S.-Y., and Darmawan, S.: 'High-index-contrast waveguides and devices', *Appl. Opt.*, 2005, **44**, pp. 3077–3086
2 Tsuchizawa, T., Yamada, K., Fukuda, H., Watanabe, T., Takahashi, J.-I., Takahashi, M., Shoji, T., Tamechika, E., Itabashi, S., and Morita, H.: 'Microphotonics devices based on silicon microfabrication technology', *IEEE J. Sel. Top. Quantum Electron.*, 2005, **11**, pp. 232–240
3 Dallesasse, J.M., Holonyak, N., Jr. Sugg, A.R., Richard, T.A., and El-Zein, N.: 'Hydrolyzation oxidation of $Al_xGa_{1-x}As$-AlAs-GaAs quantum well heterostructures and superlattices', *Appl. Phys. Lett.*, 1990, **57**, pp. 2844–2846
4 Krames, M.R., Minervini, A.D., and Holonyak, N., Jr.: 'Deep-oxide curved resonator for low-threshold AlGaAs-GaAs quantum well heterostructure ring lasers', *Appl. Phys. Lett.*, 1995, **67**, pp. 73–75
5 Luo, Y., and Hall, D.C.: 'Non-selective wet oxidation of AlGaAs heterostructure waveguides via controlled addition of oxygen', *IEEE J. Sel. Top. Quantum Electron.*, 2005, **11**, (6), pp. 1284–1291
6 Hall, D.C., Wu, H., Kou, L., Luo, Y., Epstein, R.J., Blum, O., and Hou, H.: 'Refractive index and hygroscopic stability of $Al_xGa_{1-x}As$ native oxides', *Appl. Phys. Lett.*, 1999, **75**, pp. 1110–1112
7 Roberts, J.S., David, J.P.R., Smith, L., and Tihanyi, P.L.: 'The influence of trimethylindium impurities on the performance of InAlGaAs single quantum well lasers', *J. Cryst. Growth*, 1998, **195**, pp. 668–675
8 Liang, D., Wang, J., and Hall, D.C.: 'Oxide-confined high index contrast ridge waveguide curved resonator laser diodes'. 18th Annual Meet. of IEEE Lasers and Electro-Optics Society, Sydney, Australia, 2005, paper ThZ3